Modeling of internet of things enabled sustainable environment air pollution monitoring system

Ramachandran A.[1,*], Gayathri K.[2], Aswathy R.H.[3] and Zulaikha Beevi S.[4]

[1]Department of Computer Science and Engineering, University College of Engineering, Panruti, Cuddalore-607 106, India

[2]Department of Electronics and Communication Engineering, University College of Engineering, Panruti, Cuddalore-607 106, India

[3]Department: Computer science and Engineering, KPR Institute of Engineering and Technology, Coimbatore-641407, India
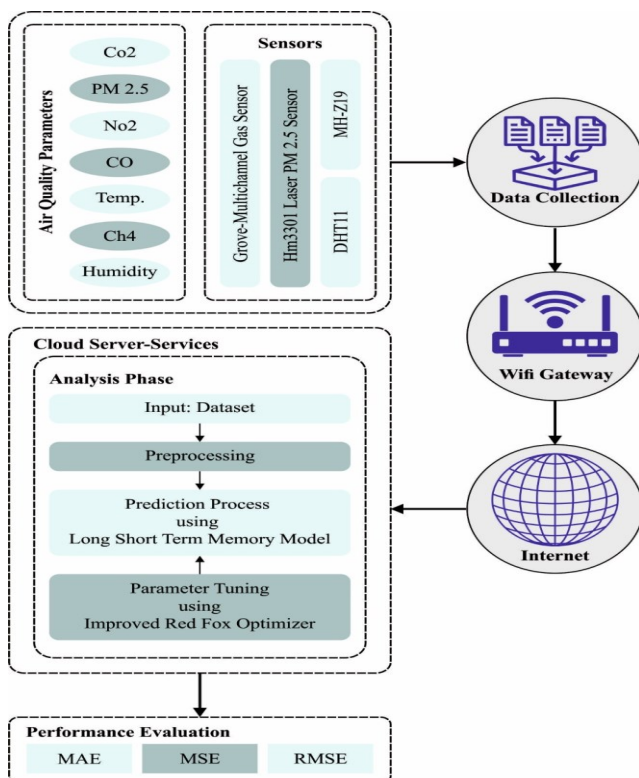
[4]Department of Computer Science and Engineering, V.S.B Engineering College, Karur, India

Graphical abstract

Abstract

Urban air pollution poses a major threat to human health. Recently, environment monitoring is become a smart environment monitoring (SEM) scheme, with the development of modern sensors and the advancements in the internet of things (IoT). Consequently, the modern method of environmental monitoring is called an SEM system, owing to the usage of wireless sensors, IoT and artificial intelligence (AI). This paper leverages IoT devices for sustainable air pollution monitoring. The presented model derives an improved red fox optimizer with a deep learning-based air pollution monitoring system (IRFODL-APMS) using IoT devices. The presented IRFODL-APMS technique makes use of different IoT devices to collect data. Besides, the IRFODL-APMS model performs a prediction process using deep learning based on long short-term memory (LSTM). At last, the IRFO technique is exploited as a hyperparameter tuning process of the LSTM model to accomplish enhanced prediction performance. The presented IRFODL-APMS model is simulated under distinct measures and the outcomes reported the enhanced predictive outcomes of the IRFODL-APMS approach over other existing models.

Keywords: Sustainability, air pollution monitoring, deep learning, red fox optimizer, internet of things

1. Introduction

Sustainable development of the entire world mainly relies upon various components namely industries, economy, agriculture, education, and much more, however, the environment was one among them that had a great contribution to the development. Health and hygiene will be considered the main elements for the progression of any country that come with a pollution-free, clean, and hazardous-free atmosphere (Amuthadevi *et al.*, 2021). Therefore, its observation is highly essential for leading a healthy life. Environment monitoring (EM) has appropriate planning and disaster management, supervising various pollutions, and efficiently addressing the difficulties that occur because of unhealthy external circumstances (Adong *et al.*, 2022). EM would deal with hazardous radiation, water pollution, weather changes, air pollution, earthquake events, and so on. The pollution can be caused by numerous components, some man-made and others because of natural calamities, and the EM plays a major role in addressing challenges precisely thereby the environment will be protected for a healthy society (Zhang and Woo, 2020).

With the rapid growth in transportation and industry, air pollution is becoming a severe issue for developing nations and gained higher attention from the public and governments (Goh *et al.*, 2021). It is known that individuals who are exposed to air pollutants for a longer period were probably suffered from respiratory diseases

Ramachandran A., Gayathri Ramachandran K., Aswathy R.H. and Zulaikha Beevi S. (2023), Modeling of internet of things enabled sustainable environment air pollution monitoring system, *Global NEST Journal*, **25**(4), 172-179.

(Dhanalakshmi, 2021). The cost of pollution harnesses might be burdensome for the government if air quality (AQ) stays to deteriorate. Thus, AQ monitoring systems were extremely helpful for effectual monitoring of air pollution before the condition turn out to be worse. Conventionally, AQ monitoring stations were large and need high costs for maintenance and installation, which limits their potentiality in densely deployed cities (Shetty *et al.*, 2020). Also, though accurate measurement outcomes are made, time-taking processes are required offline. Accordingly, AQ data could not be offered in real-time in this way. But AQ data of high spatial as well as temporal resolution in both the spatial and temporal dimensions can be extremely desired, which was the focal point of this study (Baldi *et al.*, 2022). Consequently, there will be a clear necessity for performing a prior prediction of the in-vehicle AQ which tends to alert the occupants before the AQ turn out to be worst and affects the health situation of drivers while they are driving.

Many earlier studies had mainly concentrated on categorizing hazardous gas without having the capability to forecast the upcoming condition (De Vito *et al.*, 2020). Additionally, many research works are limited to some hazardous gasses namely carbon dioxide (CO_2). In this context, there exist many techniques like regression algorithms, machine learning (ML), and artificial neural networks (ANN) that can be enforced for AQ forecasts (Ferrer-Cid *et al.*, 2021). Additionally, as the current reading of the AQ data relies upon previous data, a time-series supervised learning AQ data is utilized as the input structure. With the rapid growth of Internet-of-Things (IoT) technology, the AQ is sensed and the respective data is transferred to the servers via wireless networks like the wireless sensor networks (WSNs) (Lai *et al.*, 2022). IoT gadgets have embedded the capacity of ML and artificial intelligence (AI). The association, which is indulged in monitoring the AQ is access to the cloud via the data accumulated from numerous sensors.

This paper leverages IoT devices for sustainable air pollution monitoring. The presented model derives an improved red fox optimizer with a deep learning-based air pollution monitoring system (IRFODL-APMS) using IoT devices. The presented IRFODL-APMS technique makes use of different IoT devices to collect data. Besides, the IRFODL-APMS model performs a prediction process using DL-based long short-term memory (LSTM). At last, the IRFO algorithm is exploited as a hyperparameter tuning process of the LSTM model to accomplish enhanced prediction performance. The presented IRFODL-APMS model is simulated under distinct measures and the results reported the enhanced predictive outcomes of the IRFODL-APMS technique over other existing models.

The rest of the paper is organized as follows. Section 2 offers the related works and section 3 introduces the proposed model. Next, section 4 provides experimental validation and section 5 concludes.

2. Literature review

In Sigamani and Venkatesan (2022), developed a multi-variant regressive function as a multiple linear regressive (MLR) method to forecast air quality index (AQI) by using the correlation of two-time series–dependent parameters for meteorological and air pollutant variables. The MLR method provides high efficiency in AQI predictive model while comparing the present algorithm. The AQI is hosted on social media for initiating awareness in people and the welfare of the nation about the degradation of AQ and its related health problems. Asha *et al.* (Asha *et al.*, 2022) designed an IoT-assisted Environmental Toxicology for Air Pollution Monitoring using Artificial Intelligence technology (ETAPM-AIT) to enhance human health. For determining AQ and the classification of air pollutants, Artificial Algae Algorithm (AAA) based Elman Neural Network (ENN) system was employed as a classification that forecasts the AQ in the upcoming time stamp. The presented method has been employed as a parameter-tuning model for determining the parameter value of the ENN method.

Rahi *et al.* (Rahi *et al.*, 2022) developed a smart e-health AQ monitoring scheme that employs a meta-heuristic FA and a CSO technique for powerfully optimizing the selected feature for giving improved outcomes in the feature selection technique. Furthermore, the feature is categorized based on SVM which predicts the index level of AQ and provides improved recall and precision. Pushpam and Kavitha (Pushpam and Kavitha, 2019) propose an alternate route for the user based on the distance of all the routes and pollution status that results in a pollution-free route. By using a time series sample, the predictive analysis can be performed for PM with NN-MLP and SVM regression (SVMR) learning model. Jo and Khan (Jo and Khan, 2018) present a cost-effective, reliable, and efficient IoT scheme for monitoring AQ with the recently added feature of pollutant and assessment prediction. This scheme is encompassed transmission protocol, base station, and sensor modules, running Azure ML (AML) Studio over it.

Ferrer-Cid *et al.* (Ferrer-Cid *et al.*, 2022) developed a graph-based data reconstructed model to perform post-processing application that arises in real-time lower cost sensor deployment for monitoring air pollution. This data reconstructed model initially defines the relationship among the dissimilar network sensors through a graph learned in the measured dataset, later a signal reconstruction method is employed for reconstructing the sensor dataset. Molinara *et al.* (Molinara *et al.*, 2020) developed an IoT-ready solution to classify and detect pollutants. It can be depending on a compact and low-power combined method involving processing and sensing abilities. The sensing is comprised of a sensor array where electrical impedance measurement is accomplished using a microchip, termed SENSIPLUS, whereas the processing stage is based mostly on ML technique, embedded in resource and low-power microcontroller units, for classification purposes.

3. The proposed model

This paper has established a novel IRFODL-APMS technique for sustainable air pollution monitoring using IoT devices. The presented IRFODL-APMS technique makes use of

different IoT devices to collect data. Besides, the IRFODL-APMS model performs a prediction process using the LSTM model. At last, the IRFO system was exploited as a hyperparameter tuning process of the LSTM approach. Figure 1 represents the overall process of the IRFODL-APMS system.

3.1. IoT-based Data Collection

The IoT-based sensor begins by sensing the air pollutant and transfers the information to the cloud server's thorough examination during the data collection model. A collection of sensors employed for gathering the information connected to pollutant levels that occur from the air are determined as follows.

- Grove Multi-channel Gas Sensor: This sensor sense different gases together with Nitrogen Dioxide, Ammonia, CO, and Methane.

- MH-Z19: It is a kind of infrared gas sensor which is widely utilized to detect and measure the concentration of carbon dioxide (CO2) in air. The sensor utilizes a non-dispersive infrared (NDIR) measurement principle for detecting CO2 and has a measurement range of 400 to 5000 parts per million (ppm). It has a built-in temperature sensor for temperature compensation and an interface for communication with a microcontroller or other control unit.

- DHT11: This is a sensor usually accessible dependent upon the thermistor and humidity sensor resistive components. It can be exploited to monitor ambient temperature as well as humidity.

- HM3301 Laser PM$_{2.5}$ Sensor: It applies the diffusion of laser light to compute PM$_{2.5}$.

3.2. Z-score normalization

Z-score normalization is a normalization technique used for normalizing parameters through the standard deviation (σ) and mean (μ) values given below:

$$Z\text{-}score = \frac{(x - \mu)}{\sigma} \qquad (1)$$

3.3. Air Pollution Prediction Model

The LSTM model is exploited in this study for AQ prediction. The DNN method is a kind of feedforward NN algorithm that is a basic method for DL. DNN comprises three levels of nodes, and they follow a non-linear function, except the input nodes [18]. The study presents a backpropagation supervised learning model. This method involves the following functions and parameters: bias (b), input (x), output (y), weight (w), calculation function (α), and activation function $f(\alpha)$. All the neurons in the DNN make use of subsequent formulas [18].

$$\alpha : sum = w.x + b \qquad (2)$$

$$y : f(\alpha) = f(w \cdot x + b) \qquad (3)$$

Recurrent neural network (RNN) is a kind of DL technique used in a variety of fields namely natural language processing, computer vision, medical image diagnosis, and pattern recognition. The most prominent RNN algorithm utilized for predicting time sequence data is the LSTM approach. Figure 2 depicts the infrastructure of LSTM.
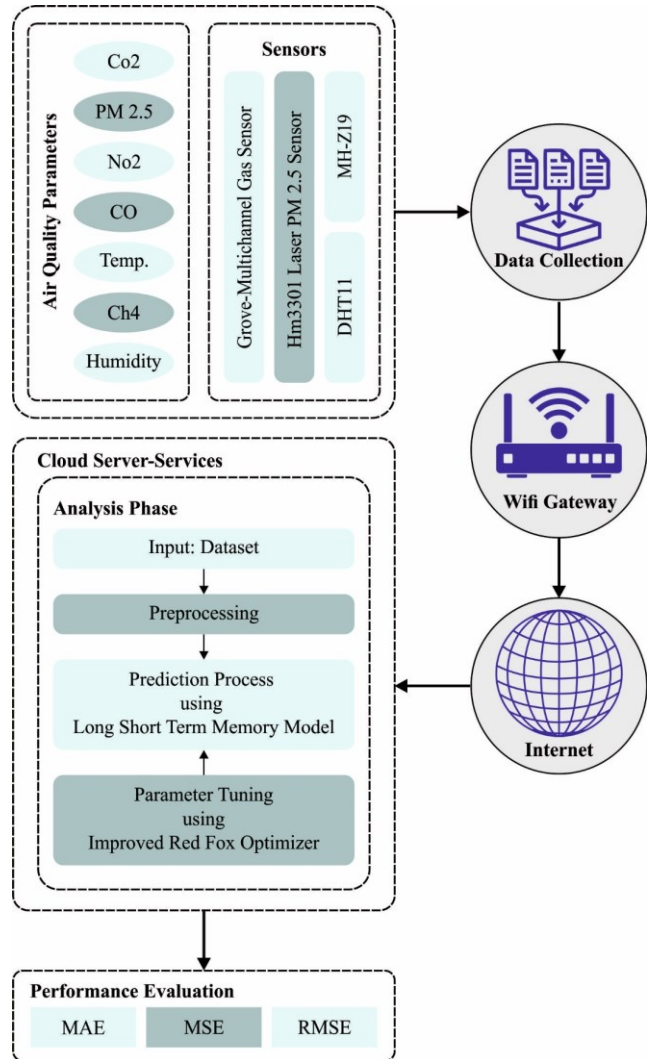

Figure 1. Overall process of IRFODL-APMS system

The LSTM and DL algorithms are better suited to estimate the time-series information when there exists a randomized-sized time step. The activating function utilized in LSTM is a logistic sigmoid. Given that input, the gate was closed and the forget gate is opened, the memory cell keep reminding of the foremost entries and thereby resolving the standard RNN problem (Aldhyani *et al.*, 2020):

$$h_t = \tan h\left(W_i \cdot h_t + w_x x_t\right) \qquad (4)$$

$$y_t = w_y \cdot w_t \qquad (5)$$

Now h_t represent the hidden layer of NN to input trained dataset(x_t). The output layer is denoted as y_t. But W_t and W_y indicate the weighted of neural cells and matrix, correspondingly. The RNN is utilized to construct the LSTM for the computing method. The LSTM comprises3 considerable variables such as output, input, and forget

gates are formulated in the subsequent equation (Aldhyani *et al.*, 2020):

$$Input\,gate: i_t = \sigma\left(W_i \cdot [h_{t-1}, x_t] + b_i\right) \tag{6}$$

$$Forget\,gate: f_t = \sigma\left(w_f \cdot [h_{t-1}, x_t] + b_f\right) \tag{7}$$

$$Output\,gate: 0_t = \sigma\left(W_0 \cdot [h_{t-1}, x_t] + b_0\right) \tag{8}$$

$$New\,memory\,cell: \overline{c}_t = \tan h\left(W_c \cdot [h_{t-1}, x_t] + b_c\right) \tag{9}$$

$$Final\,memory\,cell: C_t = f_t \times C_{t-1} + i_t \times \overline{c}_t \tag{10}$$

$$h_t = 0_t \times \tan h\left(C_t\right) \tag{11}$$

Where: i_t, f_t, and O_t: input, forget, and output gates, correspondingly. h_t: count of hidden units. σ : the logistic sigmoid function was utilized to transmit the trained dataset in the hidden unit to the output gate. $w_t\, w_t$: the weight NN. $\overline{c}$: internal memory cell was utilized to calculate in hidden unit. C_t: the internal memory. h_t: the resultant hidden units are utilized for deriving a novel memory. I, f, and O: are subscripts that represent input, forget, and output gates, correspondingly. x_t: input trained dataset. $w_f, w_o w_c$: weight vector of NN. b_f and b_o: bias vector from NN.
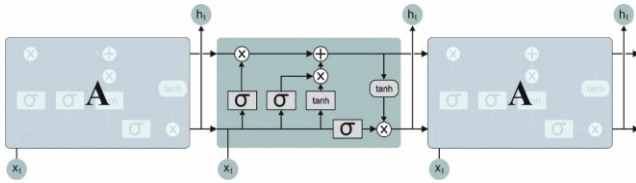

Figure 2. Framework of LSTM

3.4. Hyperparameter Tuning Model

Finally, the IRFO system was exploited as a hyperparameter tuning process of the LSTM technique. The RFO algorithm is stimulated by the behavior of red deer (PugalPriya *et al.*, 2022). Every individual (red fox) is denoted as a pixel on location (x_1, x_2) , where $x_1 \in \langle 0, w \rangle$ and $x_2 \in \langle 0, h \rangle$. The inspiration for the selective heuristic was depending on the behaviors of a herd of red foxes. The primary stage is selective of the count of each fox from the herd and it can be represented as P, then the initial population was generated, and localized was randomly chosen because of the environment size and it is evaluated as follows (PugalPriya *et al.*, 2022):

$$F(x) = \{{}^{I(x_1, x_2)}_{else\,255} < \alpha, then\,0 \tag{12}$$

where $=(x1, x2)$, and α represent a threshold value. Afterwards the assessment of each fox, the herd is arranged based on the assessed values and the one with the maximum value is chosen as the better one x^{best}. Next, every individual is moved based on the global and local movements for searching for the best location as follows (PugalPriya *et al.*, 2022):

$$x = x \pm \gamma \tag{13}$$

In Eq. (13), the sign $\pm$ is depending on the capability to go away from the image range as follows

$$\gamma = rand\left(0, d\left(x, x^{best}\right)\right) \tag{14}$$

A distance metric $d()$ is determined by using Euclidean one for two points x and y:

$$d(x, y) = \sqrt{\sum_{i=1}^{2}(x_i - y_i)^2} \tag{15}$$

Local movement depends on the decision of whether a fox needs for moving close to the possible victim or stop moving and rest. It can be modelled using the arbitrary selective of variable $\mu \in 0, 1$ [19]:

$$x = \begin{cases} \mu > 0.75 & move\,closer, \\ \mu \le 0.75 & stay\,in\,the\,current\,position \end{cases} \tag{16}$$

In such cases, if the fox decided to move, the position change can be defined by using Eq. (17)

$$x = \begin{cases} x \pm a \cdot r \cdot cos(\psi_0), if\,x = x_0 \\ x \pm a \cdot r \cdot sin(\psi_0) + a \cdot r \cdot cos(\psi_1), if\,x = x_1 \end{cases} \tag{17}$$

In Eq. (17), the coefficients $\psi_0, \psi_1 \in \langle 0, 2\pi \rangle, r \in \langle -5, 5 \rangle$ are random numbers. The r variable is an observation angle, and these values are adapted because of the great probability of changing the location of the individual. Assume that the solution space is continuous, hence a smaller variation in value leads to novel solutions. This operation is repetitive using a maximal amount of iterations T.

During this case, LOBL was employed for updating the candidate solutions in the exploration step, enlarging the search range, and supporting this technique for escaping in the local optimal (Wang *et al.*, 2022). Different models on LOBL were demonstrated mathematically as follows.

Lens imaging is a physical optics occurrence that represents the detail that but an object was placed at two or more basic focal lengths apart from the convex lens, a lesser and inverted image was created on the opposing side of the lens. To take the 1D searching space in illustration, it can be observed a convex lens with focal length f fixed at the base point O (the midpoint of the searching range in [lb, ub]). Also, an object p with height h was located on the coordinate axis, and their prediction is GX (candidate solution). The distance between the object to lens u is superior to twice f. With the lens image function, an inverted image P of heights h^* is achieved which is presented as GX^* (the reverse solution) on *the x*-axis. According to the rules of lens imaging and identical triangle, the geometrical connection attained is written as:

$$\frac{(lb + ub) / 2 - GX}{GX^* - (lb + ub) / 2} = \frac{h}{h^*} \tag{18}$$

At this point, assume that the scale factor $n = h/h^*$, the reverse solution GX was computed by transmitting as [20]:

$$GX^* = \frac{lb+ub}{2} + \frac{lb+ub}{2n} - \frac{GX}{n} \qquad (19)$$

It can be clear that if $n=1$, is simplified as the common equation of the OBL approach:

$$GX^* = lb + ub - GX \qquad (20)$$

Therefore, it is assumed the OBL approach is a peculiar case of LOBL. Concerning OBL, the latter permits obtaining dynamic reverse solutions and a wider searching range by tuning the scale factor n

Usually, it is extended to D-dimensional space:

$$GX_j^* = \frac{lb_j+ub_j}{2} + \frac{lb_j+ub_j}{2n} - \frac{GX_j}{n} \qquad (21)$$

whereas lb_j and ub_j define the lower as well as upper limits of j_{th} dimensional correspondingly, $j=1,2,...D$, GX^*_j stands for the inverse solution of GX_j from the jth dimensional.

If a novel inverse solution was created, there is no assurance that it can be continuously superior to the present candidate solution as during the gorilla place. Thus, it can be needed to estimate the fitness value of inverse as well as candidate solutions, afterwards, the fitter one is chosen for continuing participation during the succeeding exploitation stage is explained as follows [20]:

$$GX_{next} = \begin{cases} GX^*, & ifF(GX^*) < F(GX) \\ GX, & otherwise \end{cases} \qquad (22)$$

whereas GX^* implies the reverse solution, GX stands for the present candidate solutions, GX_{ext} refers to the selective gorilla for continuing the succeeding position upgrade, and F determines the fitness function of problems.

Based on mean square error (MSE) the IRFO technique derives an objective function and it is utilized for predicting the testing output of LSTM in the following.

$$MSE = \frac{\sum_{N}^{i}|y_i - \hat{y}_i|^2}{N} \qquad (23)$$

In Eq. (23), y represents the number of rounds, y_i indicates the experimental value, $\hat{y}_i$ shows the predicted values correspondingly.

4. Results and Discussion

The proposed model is simulated using Python 3.6.5 tool on PC i5-8600k, GeForce 1050Ti 4GB, 16GB RAM, 250GB SSD, and 1TB HDD. The parameter settings are given as follows: learning rate: 0.01, dropout: 0.5, batch size: 5, epoch count: 50, and activation: ReLU. In this section, the air pollution monitoring outcomes of the IRFODL-APMS model are inspected briefly.

Table 1 provides an overall prediction result of the IRFODL-APMS model on every 5 mts interval. The results indicated that the IRFODL-APMS model has reached improved prediction outcomes. For instance, on CO_2, the IRFODL-

APMS model has provided RMSE of 0.0854, MAE of 0.0523, and MSE of 0.0073, respectively. Moreover, on NO_2, the IRFODL-APMS approach has to provide an RMS of 0.0245, MSE of 0.0006, and MAE of 0.0166 correspondingly. Furthermore, on Humidity, the IRFODL-APMS system has offered me 0.0104, RMSE of 0.1020, and MAE of 0.0627 correspondingly.

Table 1. Prediction outcome analysis of IRFODL-APMS system under each 5 mts

Pollutant	MAE	MSE	RMSE
CO_2	0.0523	0.0073	0.0854
CO	0.0204	0.0013	0.0361
NO_2	0.0166	0.0006	0.0245
$PM_{2.5}$	0.0683	0.0126	0.1122
Temperature	0.0650	0.0111	0.1054
Humidity	0.0627	0.0104	0.1020

Table 2 demonstrates the overall prediction outcomes of the IRFODL-APMS approach every 15 mts interval. The outcomes referred that the IRFODL-APMS system has reached higher prediction outcomes. For samples, on CO_2, the IRFODL-APMS technique has offered MAE of 0.0548. In addition, on NO_2, the IRFODL-APMS model has provided MAE of 0.0241. Lastly, on Humidity, the IRFODL-APMS model has an obtainable MAE of 0.0617.

Table 2. Prediction result analysis of IRFODL-APMS algorithm under each 15 mts

Pollutant	MAE	MSE	RMSE
CO_2	0.0548	0.0080	0.0894
CO	0.0227	0.0027	0.0520
NO_2	0.0241	0.0014	0.0374
$PM_{2.5}$	0.0715	0.0138	0.1175
Temperature	0.0636	0.0106	0.1030
Humidity	0.0617	0.0102	0.1010

Table 3 provides an overall prediction result of the IRFODL-APMS system every 30 mts interval. The results indicated that the IRFODL-APMS technique has gained superior prediction outcomes. For samples, on CO_2 sensors, the IRFODL-APMS system has provided MAE of 0.0681, MSE of 0.0123, and RMSE of 0.1109 correspondingly. Also, on NO2-Sensors, the IRFODL-APMS model has offered an MAE of 0.0224, MSE of 0.0014, and RMSE of 0.0374 correspondingly. Moreover, on Humidity, the IRFODL-APMS system has provided MAE of 0.0552, MSE of 0.0081, and RMSE of 0.0900 respectively.

Table 3. Prediction outcome analysis of IRFODL-APMS approach under each 30 mts

Pollutant	MAE	MSE	RMSE
CO_2	0.0681	0.0123	0.1109
CO	0.0320	0.0039	0.0624
NO_2	0.0224	0.0014	0.0374
$PM_{2.5}$	0.0712	0.0135	0.1162
Temperature	0.0643	0.0108	0.1039
Humidity	0.0552	0.0081	0.0900

Table 4. Prediction result analysis of IRFODL-APMS system under each 60 mts

Pollutant	MAE	MSE	RMSE
CO_2	0.0722	0.0140	0.1183
CO	0.0368	0.0080	0.0894
NO_2	0.1071	0.0309	0.1758
$PM_{2.5}$	0.0765	0.0156	0.1249
Temperature	0.0550	0.0079	0.0889
Humidity	0.0529	0.0073	0.0854

Table 4 depictsthe overall prediction results of the IRFODL-APMS algorithm on every 60 mts interval. The results stated that the IRFODL-APMS approach has gained enhanced prediction outcomes. For instance, on CO_2, the

IRFODL-APMS system has offered an MAE of 0.0722, MSE of 0.0140, and RMSE of 0.1183 correspondingly. Along with that, on NO_2, the IRFODL-APMS technique has provided an MAE of 0.1071, MSE of 0.0309, and RMSE of 0.1758 respectively. In addition, on Humidity, the IRFODL-APMS approach has provided an MAE of 0.0529, MSE of 0.0073, and RMSE of 0.0854 correspondingly.

Figure 3 demonstrates the MAE examination of the IRFODL-APMS system with existing models. The Figure represented that the IRFODL-APMS approach has attained reduced values of MAE under all aspects and thereby affirms the enhanced prediction outcomes.

Table 5. Average analysis of IRFODL-APMS approach with existing algorithms

Avg. MAE			
Pollutant	IRFODL-APMS	ETAPMAIT	ENN	Bi-LSTM
CO_2	0.06184	0.06468	0.07418	0.08778
CO	0.02796	0.03170	0.04290	0.05370
NO_2	0.04257	0.05270	0.06460	0.07670
PM2.5	0.07190	0.11335	0.12745	0.13725
Temperature	0.06197	0.07398	0.08548	0.09818
Humidity	0.05811	0.07173	0.08113	0.09343
Avg. MSE			
Pollutant	IRFODL-APMS	ETAPMAIT	ENN	Bi-LSTM
CO_2	0.01040	0.01198	0.02248	0.03288
CO	0.00398	0.00560	0.01990	0.03220
NO_2	0.00858	0.00983	0.02323	0.03533
PM2.5	0.01388	0.01528	0.02858	0.03878
Temperature	0.01010	0.01185	0.02405	0.03585
Humidity	0.00900	0.01108	0.02478	0.03648
Avg. RMSE			
Pollutant	IRFODL-APMS	ETAPMAIT	ENN	Bi-LSTM
CO_2	0.10103	0.10945	0.14993	0.18133
CO	0.05998	0.07483	0.14107	0.17944
NO_2	0.06878	0.09915	0.15241	0.18796
PM2.5	0.11770	0.12361	0.16906	0.19693
Temperature	0.10028	0.10886	0.15508	0.18934
Humidity	0.09460	0.10526	0.15742	0.19100

Figure 4 showcases the MSE inspection of the IRFODL-APMS algorithm with existing methodologies. The figure stated that the IRFODL-APMS technique has achieved lower values of MSE under all aspects and so supports the higher prediction outcomes.

Figure 5 illustrates the RMSE investigation of the IRFODL-APMS methodology with existing approaches. The figure stated that the IRFODL-APMS method has achieved decreased values of RMSE under all aspects and thus supports improved prediction outcomes.

Table 5 provides an overall average prediction outcome of the IRFODL-APMS model [12].

Figure 6 illustrates an average MAE inspection of the IRFODL-APMS model with recent systems. The Figure inferred the enhancements of the IRFODL-APMS approach under all aspects with minimal average MAE values. For the sample, on CO_2, the IRFODL-APMS technique has reached

the least average MAE of 0.06184 while the ETAPMAIT, ENN, and Bi-LSTM models have reached superior average MAE of 0.06468, 0.07418, and 0.08778 correspondingly. Meanwhile, on NO_2, the IRFODL-APMS system has reached a minimum average MAE of 0.04257 whereas the ETAPMAIT, ENN, and Bi-LSTMtechniques have reached maximal average MAE of 0.05270, 0.06460, and 0.07670 correspondingly.

Figure 7 demonstrates an average MSE investigation of the IRFODL-APMS algorithm with recent models. The Figure stated the enhancements of the IRFODL-APMS system under all aspects with reduced average MSE values. For sample, on CO_2, the IRFODL-APMS approach has reached a minimal average MSE of 0.01040 whereas the ETAPMAIT, ENN, and Bi-LSTM models have gained improved average MSE of 0.01198, 0.02248, and 0.03288 correspondingly. In the meantime, on NO_2, the IRFODL-APMS system has obtained least average MSE of 0.00858 whereas the ETAPMAIT, ENN, and Bi-LSTMtechniques have reached

higher average MSE of 0.00983, 0.02323, and 0.03533 correspondingly.

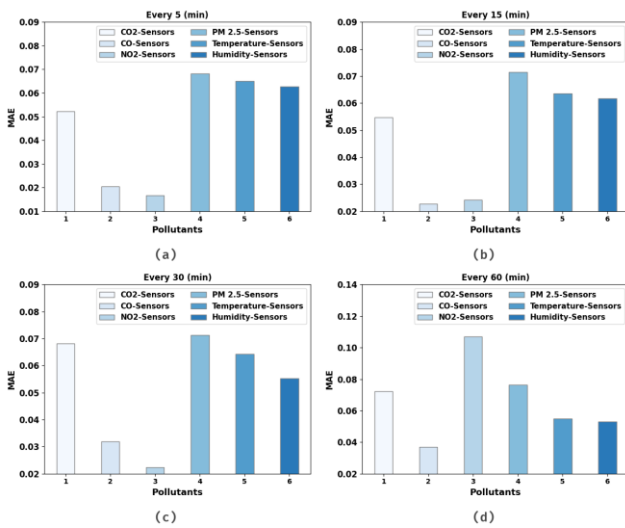improved outcomes of the IRFODL-APMS model over other models.

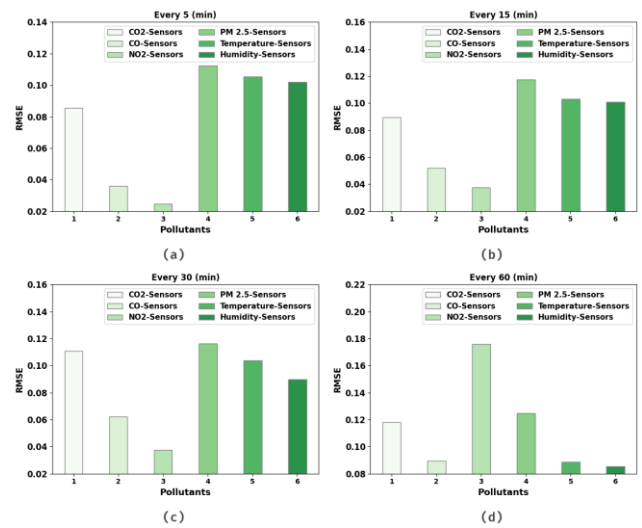**Figure 3.** MAE analysis of IRFODL-APMS approach (a) 5 mts, (b) 15 mts, (c) 30 mts, and (d) 60 mts

Figure 5. RMSE analysis of IRFODL-APMS approach (a) 5mts, (b) 15mts, (c) 30mts, and (d) 60mts
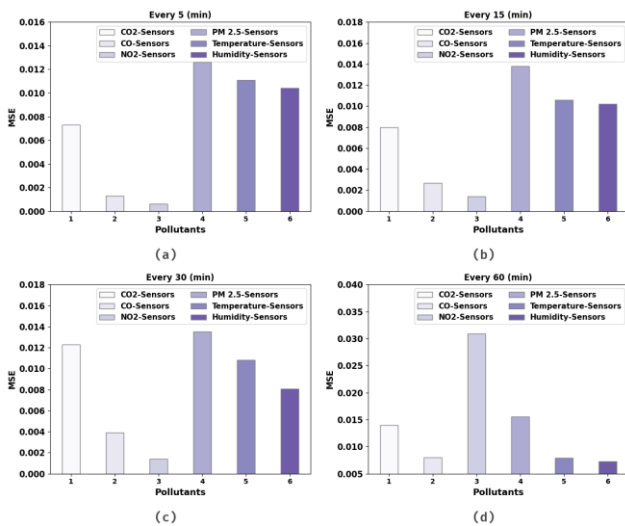

Figure 4. MSE analysis of IRFODL-APMS approach (a) 5 mts, (b) 15 mts, (c) 30 mts, and (d) 60 mts

Figure 6. Avg. MAE of IRFODL-APMS approach with recent systems

Figure 8 portrays an average RMSE examination of the IRFODL-APMS approach with recent models. The Figure revealed the enhancements of the IRFODL-APMS algorithm under all aspects with decreased average RMSE values. For instance, on CO_2, the IRFODL-APMS model has achieved decreased average RMSE of 0.10103 whereas the ETAPMAIT, ENN, and Bi-LSTMapproaches have reached maximum average RMSE of 0.10945, 0.14993, and 0.18133 correspondingly. Followed by, on NO_2, the IRFODL-APMS system has attained a minimum average RMSE of 0.06878 while the ETAPMAIT, ENN, and Bi-LSTMsystems have reached maximum average RMSE of 0.09915, 0.15241, and 0.18796 correspondingly. These results ensured the
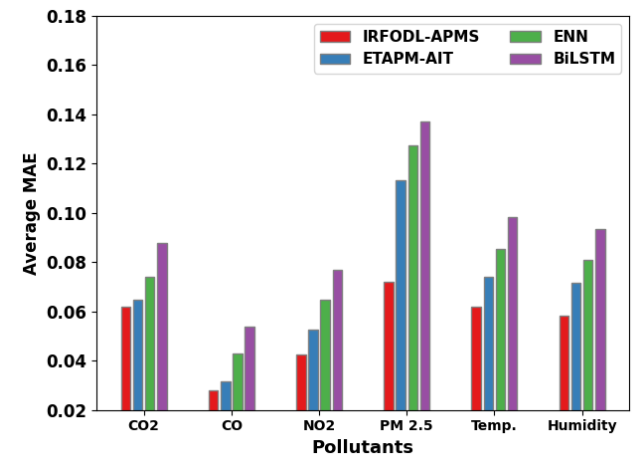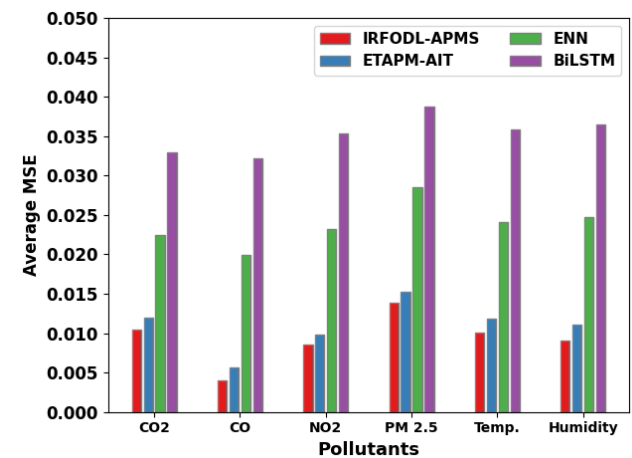

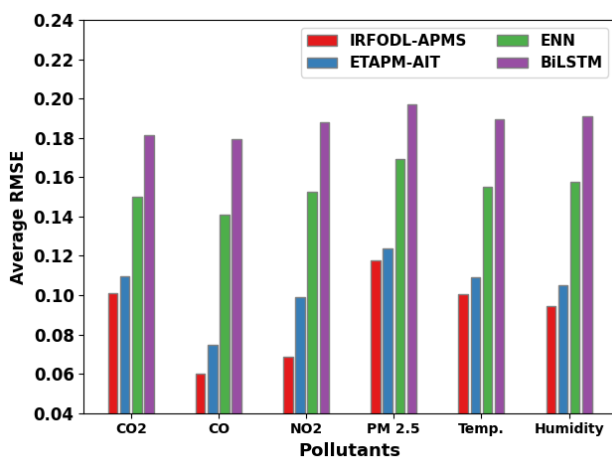**Figure 7.** Avg. MSE of IRFODL-APMS algorithm with recent systems

Figure 8. Avg. RMSE of IRFODL-APMS algorithm with recent systems

5. Conclusion

This paper has developed a novel IRFODL-APMS technique for sustainable air pollution monitoring using IoT devices. The presented IRFODL-APMS technique makes use of different IoT devices to collect data. Besides, the IRFODL-APMS model performs a prediction process using the LSTM model. At last, the IRFO technique was exploited as a hyperparameter tuning process of the LSTM system to accomplish enhanced AQ prediction performance. The presented IRFODL-APMS model is simulated under distinct measures and the results reported the improved predictive results of the IRFODL-APMS technique over other existing models. Thus, the IRFODL-APMS model appeared as an effective tool for real-time air pollution monitoring systems. In future, a hybrid DL model can be used to enhance the prediction outcomes of the IRFODL-APMS model.

References

Adong P., Bainomugisha E., Okure D. and Sserunjogi R. (2022). Applying machine learning for large scale field calibration of low-cost PM2. 5 and PM10 air pollution sensors. *Applied AI Letters*, p.e76.

Aldhyani T.H., Al-Yaari M., Alkahtani H. and Maashi M. (2020). Water quality prediction using artificial intelligence algorithms. *Applied Bionics and Biomechanics*, *2020*.

Amuthadevi C., Vijayan D.S. and Ramachandran V. (2021). Development of air quality monitoring (AQM) models using different machine learning approaches. *Journal of Ambient Intelligence and Humanized Computing*, 1–13.

Asha P., Natrayan L.B.T.J.R.R.G.S., Geetha B.T., Beulah J.R., Sumathy R., Varalakshmi G. and Neelakandan S. (2022). IoT enabled environmental toxicology for air pollution monitoring using AI techniques. *Environmental Research*, **205**, 112574.

Baldi T., Delnevo G., Girau R. and Mirri S. (2022). August. On the prediction of air quality within vehicles using outdoor air pollution: sensors and machine learning algorithms. In *Proceedings of the ACM SIGCOMM Workshop on Networked Sensing Systems for a Sustainable Society,* 14–19.

De Vito S., Di Francia G., Esposito E., Ferlito S., Formisano F. and Massera E. (2020). Adaptive machine learning strategies for network calibration of IoT smart air quality monitoring devices. *Pattern Recognition Letters*, **136**, 264–271.

Dhanalakshmi M. (2021). A survey paper on vehicles emitting air quality and prevention of air pollution by using IoT along with machine learning approaches. *Turkish Journal of Computer and Mathematics Education (TURCOMAT)*, **12**(11), 5950–5962.

Ferrer-Cid P., Barcelo-Ordinas J.M. and Garcia-Vidal J. (2021). Graph learning techniques using structured data for IoT air pollution monitoring platforms. *IEEE Internet of Things Journal*, **8**(17), 13652–13663.

Ferrer-Cid P., Barcelo-Ordinas J.M. and Garcia-Vidal J. (2022). Data reconstruction applications for IoT air pollution sensor networks using graph signal processing. *Journal of Network and Computer Applications*, 103434.

Goh C.C., Kamarudin L.M., Zakaria A., Nishizaki H., Ramli N., Mao X., Syed Zakaria S.M.M., Kanagaraj E., AbdullSukor A.S. and Elham M.F. (2021). Real-time in-vehicle air quality monitoring system using machine learning prediction algorithm. *Sensors*, **21**(15), 4956.

Jo B. and Khan R.M.A. (2018). An internet of things system for underground mine air quality pollutant prediction based on azure machine learning. *Sensors*, **18**(4), 930.

Lai W.I., Chen Y.Y. and Sun J.H. (2022). Ensemble Machine Learning Model for Accurate Air Pollution Detection Using Commercial Gas Sensors. *Sensors*, **22**(12), 4393.

Molinara M., Ferdinandi M., Cerro G., Ferrigno L. and Massera E. (2020). An end to end indoor air monitoring system based on machine learning and SENSIPLUS platform. *IEEE Access*, **8**, 72204–72215.

PugalPriya R., SaradadeviSivarani T. and GnanaSaravanan A. (2022). Deep long and short term memory based Red Fox optimization algorithm for diabetic retinopathy detection and classification. *International Journal for Numerical Methods in Biomedical Engineering*, **38**(3), p.e3560.

Pushpam V.E. and Kavitha N.S. (2019). January. Iot enabled machine learning for vehicular air pollution monitoring. In *2019 International Conference on Computer Communication and Informatics (ICCCI)* 1–7. IEEE.

Rahi P., Sood S.P. and Bajaj R. (2022). Meta-Heuristic with Machine Learning-Based Smart e-Health System for Ambient Air Quality Monitoring. In *Recent Innovations in Computing* 501–519. Springer, Singapore.

Shetty C., Sowmya B.J., Seema S. and Srinivasa K.G. (2020). Air pollution control model using machine learning and IoT techniques. In *Advances in Computers,* **117**, 1, 187–218. Elsevier.

Sigamani S. and Venkatesan R. (2022). Air quality index prediction with influence of meteorological parameters using machine learning model for IoT application. *Arabian Journal of Geosciences*, **15**(4), 1–12.

Wang Z., Ding H., Yang Z., Li B., Guan Z. and Bao L. (2022). Rank-driven salp swarm algorithm with orthogonal opposition-based learning for global optimization. *Applied Intelligence*, **52**(7), 7922–7964.

Zhang D. and Woo S.S. (2020). Real time localized air quality monitoring and prediction through mobile and fixed IoT sensing network. *IEEE Access*, **8**, 89584–89594.